Seasonal measurements of OH, NO_x, and $J(O^1D)$ at Mace Head, Ireland

H. Berresheim,[1] J. McGrath,[1] M. Adam,[1] R.L. Mauldin III,[2,3] B. Bohn,[4] and F. Rohrer[4]

Received 18 January 2013; revised 4 March 2013; accepted 10 March 2013; published 28 April 2013.

[1] Measurements of atmospheric OH concentrations were conducted between August 2010 and July 2011 at Mace Head showing maximum daytime values of 0.21 $(\pm 0.25) \times 10^6\,cm^{-3}$ in winter and 2.26 $(\pm 1.37) \times 10^6\,cm^{-3}$ in summer. Plots of OH versus ozone photolysis frequency, $J(O^1D)$, exhibited strong linear correlations with slopes of 1.06 $(\pm 0.05) \times 10^{11}\,cm^{-3}\,s$ ($R = 0.75$) in clean marine air and 1.31 $(\pm 0.04) \times 10^{11}\,cm^{-3}\,s$ ($R = 0.79$) in mixed marine/continental air. Surprisingly, no significant difference in the former correlation was found between low and high tide periods. NO and NO_2 levels in air from the marine sector (190–300°) were typically below the detection limit (30 pptv and <200 pptv, respectively). In the land sector, NO mixing ratios <50 pptv dominated most of the time, suggesting that the atmospheric oxidation efficiency in this region is predominantly characterized by primary OH sources in a low NO_x environment. **Citation:** Berresheim, H., J. McGrath, M. Adam, R. L. III Mauldin, B. Bohn, and F. Rohrer (2013), Seasonal measurements of OH, NO_x, and $J(O^1D)$ at Mace Head, Ireland, *Geophys. Res. Lett.*, *40*, 1659–1663, doi:10.1002/grl.50345.

1. Introduction

[2] The need for direct measurements of the hydroxyl radical, OH, and a systematic network-based monitoring of the atmospheric oxidizing efficiency has been clearly recognized, e.g., *IPCC* [2007]. The first and to this date unprecedented long-term measurements of atmospheric OH (and sulfuric acid) concentrations have been conducted at the Global Atmosphere Watch (GAW) observatory Hohenpeissenberg in rural southern Germany [*Berresheim et al*., 2000]. The results from the first 5 years of measurements (1999–2004) showed a surprisingly strong correlation of OH levels with solar UVB radiation via the ozone photolysis frequency, $J(O^1D)$, with a distinct slope in the $OH/J(O^1D)$ relation [*Rohrer and Berresheim*, 2006]. This relation was proposed to be characteristic for the background continental atmosphere on a spatial scale of synoptic weather patterns. *Rohrer and Berresheim* [2006] further suggested that $OH/J(O^1D)$ relations may be equally strong but characteristically different over other regions with different levels of air pollution such as in the marine atmosphere.

[3] A suitable GAW station for conducting such measurements in the northern hemisphere is the Mace Head Atmospheric Research Station on the west coast of Ireland (53.33°N, 9.9°W). During 52% of the year on average [*O'Connor et al*., 2008], the station receives background oceanic air from the North and South Atlantic regions. At other times, it is impacted by continental air masses from Western Europe and by regional emissions from Ireland and the United Kingdom. Since 1997, field campaigns including OH measurements have been conducted at Mace Head by various groups [*Heard et al*., 2006; *Smith et al*., 2006; *Creasey et al*., 2002; *Berresheim et al*., 2002; *Savage et al*., 2001]. However, measurements were made only during spring and summer periods, and the results still showed significant discrepancies between modeled and measured OH levels [*Sommariva et al*., 2006].

[4] In the present work, we report the first seasonal measurements of OH, nitrogen oxides, and $J(O^1D)$ at Mace Head. We provide a preliminary analysis of OH variance on different time scales and compare $OH\text{-}J(O^1D)$ relations in air advected through the marine and land sectors, respectively.

2. Experiment

[5] A chemical ionization mass spectrometer (CIMS) with advanced ion guide optics and compact design was put into operation at Mace Head in 2010 for long-term measurements of OH concentrations in the coastal atmosphere. Similar prototype instruments have been described in detail previously [*Petäjä et al*., 2009; *Mauldin et al*., 1998]. Briefly, OH is measured as the resulting $H^{34}SO_4^-$ ion signal after addition of $^{34}SO_2$, which reacts with OH in the sample air, followed by ion exchange of the oxidation product $H_2^{34}SO_4$ with NO_3^- ions. The NO_3^- ions are produced in a sheath flow which passes by a radioactive alpha source (^{241}Am). The CIMS was installed on the top floor of one of the laboratory buildings with the air inlet approximately 5 m above ground (approximately 10 m above mean sea level) and 40 cm in front of the outer wall facing west towards the ocean. Distance to the water ranged between 80 m at high tide and 180 m at low tide. Exhaust air containing traces of propane and sulfur dioxide was disposed through long tubing at least 50 m away from the station.

[6] Continuous measurements started in August 2010, with interruptions mainly due to periods of severe weather conditions, calibration, or instrument maintenance. In typical operation mode, one OH measurement cycle is completed after 30 s and then repeated 10 times to obtain a 5 min average value. Instrument parameters and additional compounds such as sulfuric acid are measured over further selectable time intervals. Based on the NO_3^- ion statistics, we estimate the precision of the 5 min integrated OH measurements to be

[1]School of Physics and Center for Climate and Air Pollution Studies, National University of Ireland Galway, Galway, Ireland.
[2]Department of Physics, University of Helsinki, Helsinki, Finland.
[3]Atmospheric and Oceanic Sciences, University of Colorado, Denver, Colorado, USA.
[4]Institute for Energy and Climate Research (IEK-8), Research Center Jülich, Jülich, Germany.

Corresponding author: H. Berresheim, School of Physics and Center for Climate and Air Pollution Studies, National University of Ireland Galway, Ireland. (harald.berresheim@nuigalway.ie)

©2013. American Geophysical Union. All Rights Reserved.
0094-8276/13/10.1002/grl.50345

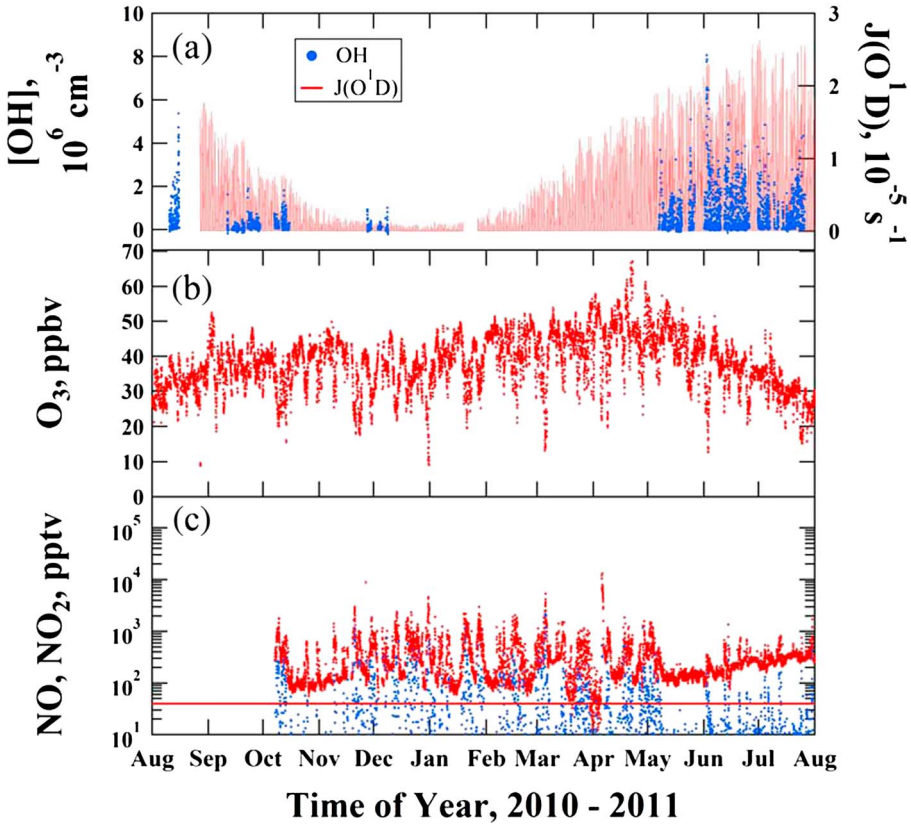

Figure 1. Time series of atmospheric concentrations of (a) OH and $J(O^1D)$, (b) O_3, and (c) NO (blue) and NO_2 (red) measured at Mace Head between August 2010 and August 2011. Data are averaged for 5 min (in Figure 1a) and for 1 h (in Figures 1b and 1c), respectively. Corresponding NO and NO_2 detection limits were 10 pptv and 40 pptv (red line), respectively.

$\sigma_{OH} = 6.6 \times 10^4\,cm^{-3} + 6.6 \times 10^{-2}$ [OH]. The overall detection limit for OH with the Mace Head CIMS instrument is estimated to be $1.3 \times 10^5\,cm^{-3}$ for 5 min signal integration with an estimated accuracy of 40% (both 2σ). Calibrations were conducted approximately every 3 months as described by *Berresheim et al.* [2000].

[7] Nitrogen oxides (NO, NO_2) were monitored with a Thermo Systems 42i trace level instrument based on the ozone chemiluminescence reaction with NO. The instrument was modified by replacing the standard NO_2 molybdenum converter with a blue light converter (BLC) for selective interference-free measurements of NO_2 (Air Quality Design, Golden, USA). Only data generated with the BLC converter are included in the present paper, with measurements starting in October 2010. Calibrations were performed on a 2–3 month basis with standards generated from a NO_2 Dynacal permeation tube (VICI-Metronics) contained in a self-built oven which was kept at 40°C under a pure zero air flow. NO was generated by passing the NO_2 calibration mixture through a cartridge containing $FeSO_4$. A short Teflon line for ambient air sampling (maximum 5 m length) was used with the inlet at the same height as that of the CIMS inlet. Detection limits for NO and NO_2 based on 5 min signal averaging and 2σ uncertainty are estimated to be 30 and 120 parts per trillion by volume (pptv), respectively.

[8] Ozone mixing ratios at 10 m above ground were measured continuously with a Thermo Systems 49i instrument as part of the basic operational program at Mace Head. Two filter radiometers for measuring photolysis frequencies of ozone, $J(O^1D)$, and of nitrogen dioxide, $J(NO_2)$, were deployed in September 2010 on top of a 10 m tower next to the laboratory building. Both were exchanged with recalibrated systems on a semiannual basis. Details of the measurement principles and performance of the radiometers have been given by *Bohn et al.* [2008].

3. Results and Discussion

[9] Figure 1a shows the time series of OH concentrations and ozone photolysis frequencies, $J(O^1D)$, measured over the entire 2010–2011 period, with each series representing 5 min signal integration values. From the total of 3219 OH values shown in Figure 1a, approximately half (52%) were obtained in the marine wind sector (190–300°), which also includes a coastal sector (190–200° and 290–300°) roughly representing the north-south orientation of the shoreline in the vicinity of Mace Head.

[10] As expected, OH levels peaked during local noontime hours, with the corresponding times mainly depending on cloud coverage. From the above data set, approximate monthly OH maximum values (peak averages) were calculated. Only those months were considered in this estimate during which OH had been measured on at least 3 days with the mean values determined for the midday period of 1000–1400 h (UTC). The results are shown in Table 1. Clearly, the seasonal variation of atmospheric OH levels is evident from the data suggesting noontime peak values of $2 \times 10^6\,cm^{-3}$ in the summer months and 1 order of magnitude lower levels in winter.

[11] Nighttime OH levels were measured during a total of 65 nights between local sunset and sunrise showing average

Table 1. Mean Monthly OH Concentrations and Standard Deviations[a]

	$[OH]_{peak}$	n
2010		
August	1.93 (±1.56)	6
September	0.26 (±0.28)	15
October	0.40 (±0.27)	7
November	0.24 (±0.26)	4
December	0.21 (±0.25)	4
2011		
May	1.12 (±0.85)	15
June	2.26 (±1.37)	24
July	1.17 (±1.02)	23

[a]During peak daylight hours (1000–1400 UTC) in 10^6 cm^{-3} (n = number of days).

values of 8.6×10^4 cm^{-3} and 9.8×10^4 cm^{-3} in air advected from the marine and land sectors, respectively. These values are not significantly different from the detection limit. Average 24 h OH concentrations weighted for day time and nighttime periods were estimated to be 7.8 $(\pm 4.3) \times 10^5$ cm^{-3} for summer (June/July) and 1.1 $(\pm 0.6) \times 10^5$ cm^{-3} for winter (November/December). The summer average determined here compares well with the 9.1×10^5 cm^{-3} mean reported previously by *Smith et al*. [2006]. However, it is significantly higher than the 2.5×10^5 cm^{-3} measured in a campaign in June 1999 [*Berresheim et al*., 2002] with mainly overcast conditions and unusually low temperatures.

[12] Figures 1b and 1c show the concurrent atmospheric O_3, NO, and NO_2 mean hourly mixing ratios. Average ozone levels were approximately 40 ppbv in agreement with the long-term record at Mace Head [*Tripathi et al*., 2010]. Calibrated NO and NO_2 measurements started in October 2010. The mixing ratios shown in Figure 1c clearly distinguish individual (moderate) pollution events which mainly occurred in winter due to emissions from domestic heating in the land sector area near the station. Background NO levels in the marine atmosphere were around or below the detection limit of 30 pptv (5 min signal integration) and ranged between approximately 100 and 200 pptv for NO_2. Overall average levels during the entire measurement period were 28 pptv NO (daytime) and 350 pptv NO_2.

[13] In Figure 2, we present the correlation between OH and $J(O^1D)$, which shows the importance of photolysis processes as the dominant source of hydroxyl in the study area. The data set has been divided according to air mass advection from the marine sector (Figure 2, top panel) and the land sector (Figure 2, bottom panel) as previously

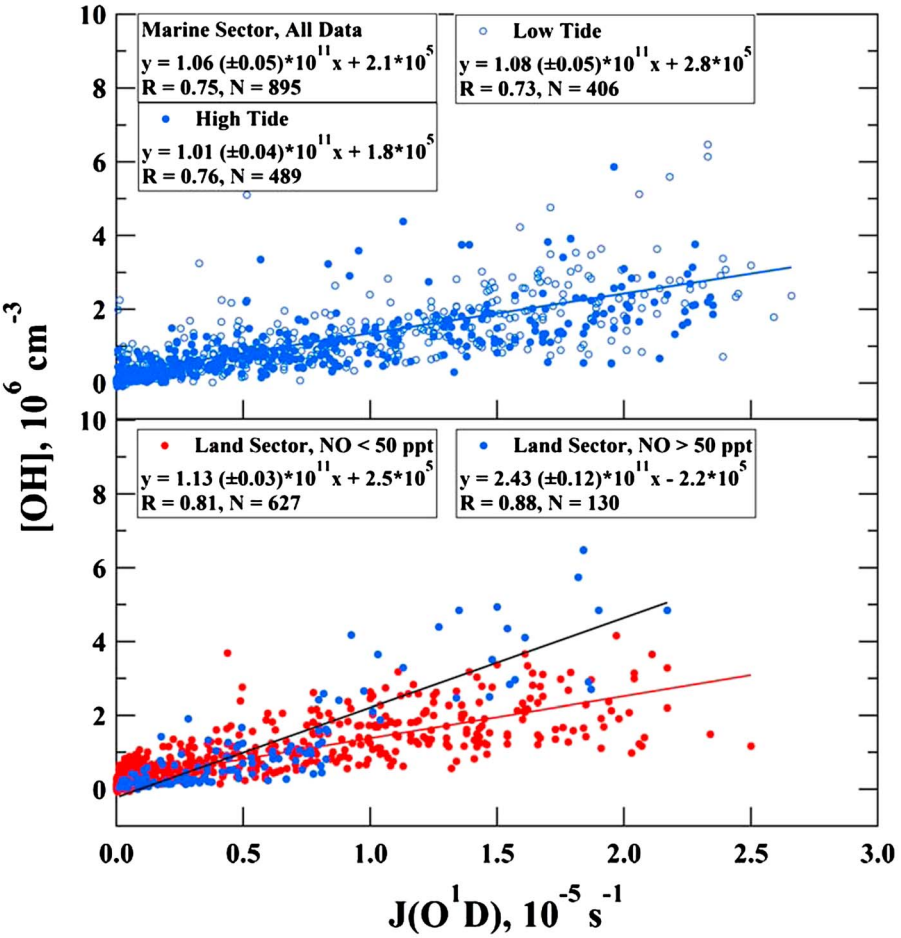

Figure 2. Correlation between measured OH concentrations and ozone photolysis frequency, $J(O^1D)$, in air from marine sector (top panel), divided by 6 h periods of low and high tide (open and filled symbols, respectively), and from land sector (bottom panel), divided into subsets of measurements during conditions of low (<50 pptv) and high (>50 pptv) NO mixing ratios.

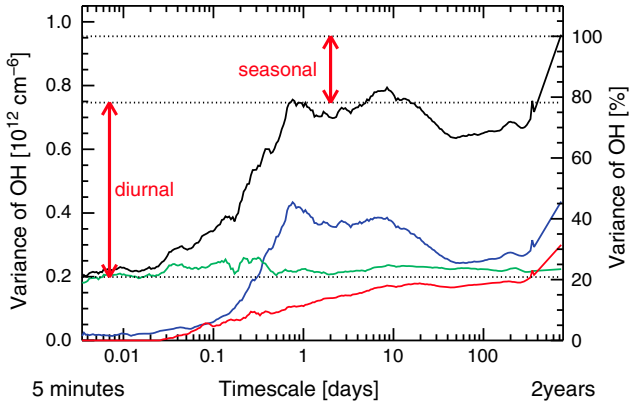

Figure 3. Variance analysis of OH and J(O^1D) observations shown in Figure 2. For details of this technique, see *Rohrer and Berresheim* [2006]. The black line denotes total variance of OH, the blue line the part of OH variance which correlates with J(O^1D), and the green line the contribution of noise to the OH signal. The red line denotes the unassigned variance calculated as the difference of the total variance minus the contributions from J(O^1D) correlation and noise. The reduction of variance in the range 20 to 300 days is probably caused by gaps in the data set.

defined. Furthermore, the marine data are classified by periods of low and high tide. The correlation found for all marine sector data was high (R = 0.75, N = 895) with a slope of 1.06 (±0.05) × 10^{11} cm^{-3} s. No significant difference was found for the OH-J(O^1D) relationship between low and high tide periods. This was also observed previously during the 1999 campaign with a slope of 0.8 × 10^{11} cm^{-3} s (H. Berresheim, unpublished data, 1999). This result is quite surprising as one might have expected major influences on ambient OH concentrations from enhanced biogenic emissions of reactive iodine, sulfur, and organic compounds during low tide and subsequent fast reactions involving OH triggering intensive particle nucleation events [e.g., *O'Dowd and de Leeuw*, 2007]. Although anticorrelations between ultrafine particle and OH concentrations were occasionally observed at low tide, they were restricted to the early phases of new particle formation events and detectable only at elevated OH levels during noontime hours (*Berresheim et al.*, 2002).

[14] A significantly higher slope in the OH-J(O^1D) relationship was found for the land sector data shown in Figure 2 (bottom panel) with 1.31 (±0.04) × 10^{11} cm^{-3} s overall, a value which, however, was still about a factor of 2 lower than previous findings for (background) continental air masses [*Rohrer and Berresheim*, 2006]. Iterative inclusion of these data based on corresponding NO levels showed that the most significant increase in the regression slope was noticeable when NO levels increased above 50 pptv. Therefore, the data in Figure 2 (bottom panel) have been subdivided into one set corresponding to NO < 50 pptv (low NO_x regime) and the other set for NO > 50 pptv (maximum approximately 300 pptv). The former set includes 83% of all land sector data and shows a slope (1.13 × 10^{11} cm^{-3} s) close to the value found for the marine sector (Figure 2, top panel). The elevated slope of the second data set (2.43 × 10^{11} cm^{-3} s) was mainly due to moderately polluted air prevailing on 8 days in June and July 2011 (high data points in Figure 2, bottom panel). We conclude that, apart from sporadic exceptions, the contribution by the NO + HO_2 recycling reaction to the overall OH budget at Mace Head is minor compared to the OH primary source by ozone photolysis. Also, in view of the relatively low NO_x (=NO + NO_2) levels observed in air from the land sector, we estimate contributions from HONO photolysis to ambient OH levels to be generally negligible.

[15] Linear OH/J(O^1D) relationships with similar slopes in clean to moderately polluted marine air have previously been reported by *Vaughan et al.* [2012] for Cape Verde Island (0.90–1.30 × 10^{11} cm^{-3} s) and *Brauers et al.* [2001] for measurements made between 5°N and 40°S during a cruise on the Atlantic Ocean (1.37 × 10^{11} cm^{-3} s). Therefore, with reference to the various campaigns discussed by *Rohrer and Berresheim* [2006], we conclude that OH/J(O^1D) linear slopes for marine air masses are on the order of 0.8–1.3 × 10^{11} cm^{-3} s, whereas in continental air masses these can assume values of 2.0 × 10^{11} cm^{-3} s and higher depending on the corresponding NO_x pollution regime.

[16] Figure 3 shows the variance analysis of the 30 s time-resolved OH and J(O^1D) data based on the method described by *Rohrer and Berresheim* [2006]. Very similar to the results obtained at the Meteorological Observatory Hohenpeissenberg, the Mace Head 30 s data set shows a 20% contribution of instrument noise and 50% contribution of the diurnal behavior of photolysis processes to the total variance of OH observations. The variance at small time scales is fully consistent with the precision estimate given in section 2 derived from counting statistics. Counting statistics would yield a minimum variance of 0.2 × 10^{12} cm^{-6}, which is the value at small time scales in Figure 3. This analysis shows that there are no atmospheric contributions to the variability of OH below time scales of 1 h at Mace Head.

[17] The two known contributions to total variance leave 30% unexplained. This unexplained variance appears to be predominantly generated on time scales from 1 h to 10 days comprising the impact of atmospheric chemistry on OH, for example, reactions of nitrogen oxides and volatile organic compounds (VOCs). Subtracting the contribution of instrument noise, Figure 3 shows that a simple linear parameterization of OH as a function of J(O^1D) describes atmospheric OH levels at Mace Head within a precision of 38% without taking any detail of photochemistry into account.

[18] To compare the observed OH levels to the current theory of atmospheric chemistry, we performed model calculations using a simple CO-CH_4 chemistry derived from RACM-MIM-GK as described in *Hofzumahaus et al.* [2009] and *Lu et al.* [2012]. These model calculations were performed for typical summer time conditions at Mace Head to obtain the model calculated slope of OH versus J(O^1D). Assuming the following values for marine conditions, J(O^1D) = 2 × 10^{-5} s^{-1}, J(NO_2) = 8 × 10^{-3} s^{-1}, O_3 = 36 ppbv, CH_4 = 1900 ppbv, H_2 = 550 ppbv, CO = 120 ppbv, HCHO = 0.4 ppbv, H_2O_2 = 1 ppbv, T = 14.2°C, and RH = 76%, the model yields a OH versus J(O^1D) linear regression slope of 1.4 × 10^{11} cm^{-3} s for NO = 0 pptv consistent with the observed slope for the marine sector and 3.7 × 10^{11} cm^{-3} s for NO = 50 pptv, respectively. To be more consistent with the latter result, an additional OH reactant equivalent to 3 ppmv of CH_4 is needed to enhance total OH reactivity k_{OH} from 1.56 s^{-1} to 2.13 s^{-1}. For this reactivity, a 50 pptv NO

mixing ratio yields a slope of $2.7 \times 10^{11}\,\mathrm{cm}^{-3}\,\mathrm{s}$, which is consistent with the experimental results obtained for the land sector with NO > 50 pptv (Figure 2, bottom panel).

4. Conclusions

[19] In this work, we report the first long-term OH measurements in the northern midlatitude marine atmosphere. The results confirm that the atmospheric oxidation efficiency in the coastal region of Mace Head, Ireland, is rarely affected by elevated NO_x pollution. For this low NO_x regime (NO typically <50 pptv), a strong correlation was found between OH levels and the ozone photolysis frequency, $J(O^1D)$, with a linear regression slope typical for clean marine air as suggested from previous field campaigns. On the other hand, the sensitivity of prevailing OH concentrations even for relatively low levels of air pollution advected to the study area could be demonstrated during short periods marked by elevated levels of NO_x. Surprisingly, no significant influence of the tidal cycle (with presumably substantial emissions of reactive biogenic compounds at low tide) or systematic influences of new particle formation events on atmospheric OH levels were observed.

[20] **Acknowledgments.** We would like to thank F. Eisele for helpful discussions and Science Foundation Ireland (grant 09/RFP/GEO2176) and EPA Ireland (grant 2007-INF-12-S5) for financial support (4/SU-AB-1924).

References

Berresheim, H., T. Elste, C. Plass-Dülmer, F. L. Eisele, and D. J. Tanner (2000), Chemical ionization mass spectrometer for long-term measurements of atmospheric OH and H_2SO_4, *Int. J. Mass Spectrom.*, *202*, 91–109.

Berresheim, H., T. Elste, H. G. Tremmel, A. G. Allen, H.-C. Hansson, K. Rosman, M. DalMaso, J. M. Mäkelä, M. Kulmala, and C. D. O'Dowd (2002), Gas-aerosol relationships of H_2SO_4, MSA, and OH: Observations in the coastal marine boundary layer at Mace Head, Ireland, *J. Geophys. Res.*, *107*(D19), 8100. doi:10.1029/2000JD000229.

Bohn, B., et al. (2008), Photolysis frequency measurement techniques: Results of a comparison within the ACCENT project, *Atmos. Chem. Phys.*, *8*, 5373–5391.

Creasey, D. J., D. E. Heard, and J. D. Lee (2002), Eastern Atlantic Spring Experiment 1997 (EASE97) 1, measurements of OH and HO_2 concentrations at Mace Head, Ireland, *J. Geophys. Res.*, *107*, D10, doi:10.1029/2001JD000892.

Heard, D. E., et al. (2006), The North Atlantic Marine Boundary Layer Experiment (NAMBLEX). Overview of the campaign held at Mace Head, Ireland, in summer 2002, *Atmos. Chem. Phys.*, *6*, 2241–2272.

Hofzumahaus, A., et al. (2009), Amplified trace gas removal in the troposphere, *Science*, *324*, 1702–1704.

IPCC (2007), Intergovernmental Panel on Climate Change, working group 1, Climate change 2007: The physical science basis of climate change, Fourth Assessment Report AR4, Chapter 2.3.5, *Trends in the hydroxyl free radical*, P. Forster and W. Ramaswamy (lead authors), World Meteorological Organization, Geneva.

Lu, K. D., et al. (2012), Observation and modelling of OH and HO_2 concentrations in the Pearl River Delta 2006: A missing OH source in a VOC rich atmosphere, *Atmos. Chem. Phys.*, *12*, 1541–1569.

Mauldin, R., III, G. Frost, G. Chen, D. Tanner, A. Prevot, D. Davis, and F. Eisele (1998), OH measurements during the First Aerosol Characterization Experiment (ACE 1): Observations and model comparisons, *J. Geophys. Res.*, *103*, 16713–16729.

O'Connor, T. C., S. G. Jennings, and C. D. O'Dowd (2008), Highlights from 50 years of aerosol measurements at Mace Head, *Atmos. Res.*, *90*, 338–355.

O'Dowd, C. D., and G. de Leeuw (2007), Marine aerosol production: A review of the current knowledge, *Phil. Trans. R. Soc. A*, *365*, 1753–1774.

Petäjä, T., R. L. III Mauldin, E. Kosciuch, J. McGrath, T. Nieminen, P. Paasonen, M. Boy, A. Adamov, T. Kotiaho, and M. Kumala (2009), Sulfuric acid and OH concentrations in a boreal forest site, *Atmos. Chem. Phys.*, *9*, 7435–7448.

Rohrer, F., and H. Berresheim (2006), Strong correlation between levels of tropospheric hydroxyl radicals and solar ultraviolet radiation, *Nature*, *442*, 184–187.

Savage, N. H., R. M. Harrison, P. S. Monks, and G. Salisbury (2001), Steady-state modelling of hydroxyl radical concentrations at Mace Head during the EASE '97 campaign, May 1997, *Atmos. Environ.*, *35*, 515–524.

Smith, S. C., J. D. Lee, W. J. Bloss, G. P. Johnson, T. Ingham, and D. E. Heard (2006), Concentrations of OH and HO_2 radicals during NAMBLEX: Measurements and steady state analysis, *Atmos. Chem. Phys.*, *6*, 1435–1453.

Sommariva, R., et al. (2006), OH and HO_2 chemistry during NAMBLEX: Roles of oxygenates, halogen oxides and heterogeneous uptake, *Atmos. Chem. Phys.*, *6*, 1135–1153.

Tripathi, O. P., S. G. Jennings, C. D. O'Dowd, L. Coleman, S. Leinert, B. O'Leary, E. Moran, S. J. O'Doherty, and T. G. Spain (2010), Statistical analysis of eight surface ozone measurement series for various sites in Ireland, *J. Geophys. Res.*, *115*, D19302, doi:10.1029/2010JD014040.

Vaughan, S., et al. (2012), Seasonal observations of OH and HO_2 in the remote tropical marine boundary layer, *Atmos. Chem. Phys.*, *12*, 2149–2172.